Supporting information

Carbon quantum dots@mesoporous silicon composite-based fluorescent probe for chlortetracycline hydrochloride and gentamicin

Lina Gao and Jing Wang*

School of Chemistry and Chemical Engineering, Guangxi University, Nanning 530004, PR China

Corresponding author, e–mail: wjwyj82@gxu.edu.cn

Table S1. Basic information of used antibiotics

Types of antibiotics	Name of antibiotics	Structure
Penicillin antibiotic	Penicillin G potassium (PEN)	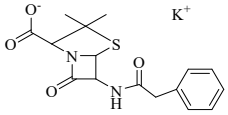
Macrolide antibiotics	Erythromycin(ERM)	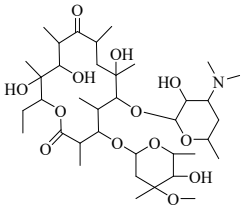
	Clarithromycin(CLA)	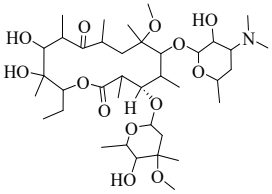
	Roxithromycin(ROX)	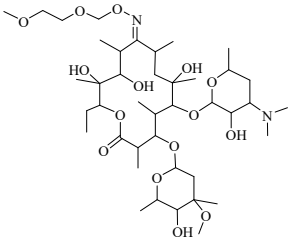
Sulfonamide antibiotics	Sulfathiazole(STZ)	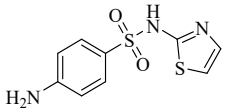
	Sulfachloropyridazine(SCP)	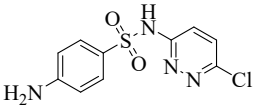

	Sulfamethoxypyridazine(SMP)	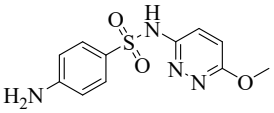
	Sulfamethizol(SMT）	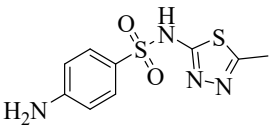
	Sulfamerazine(SMR)	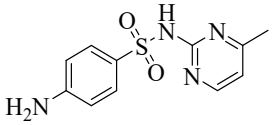
	Sulfamethoxazole(SMZ)	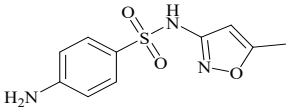
	Sulfisoxazole(SIZ)	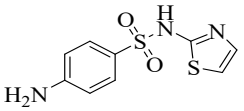
Tetracycline antibiotics	Tetracycline hydrochloride(TC)	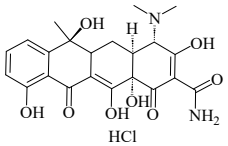
	Oxytetracycline Hydrochloride(OTC)	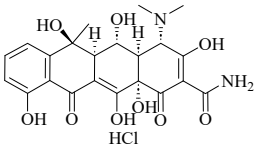
	Chlortetracycline hydrochloride(CTC)	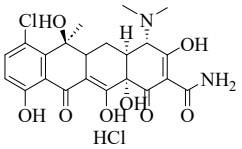
Aminoglycoside antibiotics	Gentamicinsulfate(GTM)	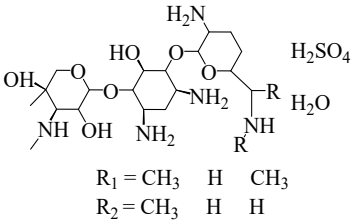
	Kanamycin sulfate(KNM)	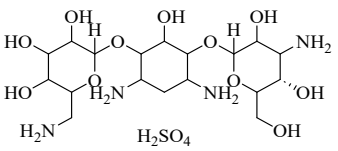

Streptomycin sulfate(STR)	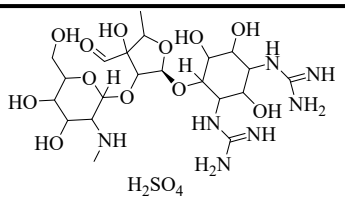

Table S2.BET specific surface area (S_{BET}), total pore volume (V_{total}), and mean pore size (D_{BJH}) of CDs@SBA-15

Sample	S_{BET} (m^2/g)	V_{total} (cm^3/g)	D_{BJH} (Å)
SBA–15[S1]	780.03	1.37	98.59
CDs@SBA-15	434.8	0.95	87.1

Table S3. Fluorescence decay parameters of CDs@SBA-15 in the absence and presence of GTM and CTC

Sample	T_1(ns)	T_2(ns)	B_1	B_2	τ(ns)
CDs@SBA-15	2.12	8.71	0.0936	0.0197	3.2681
CDs@SBA-15-GTM	2.71	1.06	0.0834	0.0209	4.2892
CDs@SBA-15-CTC	1.84	8.23	0.0990	0.0197	2.9019

Table S4. The LUMO and HOMO energy levels of GTM and CTC

Sample	LUMO	HOMO
GTM	0.696	-5.799
CTC	-2.032	-6.044

Table S5. Performance comparison of CDs@SBA-15 with the reported detection methods

Materials	Method applied	Antibiotic type	Detection mode	LOD	Refs.
CDs@SBA-15	Fluorescence detection	GTM	Turn on	29 nM	This work
GQD and Ag NPs	Fluorescence detection	GTM	Turn on	0.493 μM	[S2]
Au@CQDs	Fluorescence detection	GTM	Turn on	133 nM	[S3]
N，S-CDs	Fluorescence detection	GTM	Turn off	0.42 μM	[S4]
CdS@PCN-224	PEC	GTM	-	0.158 nM	[S5]
AbGEN	SPR	GTM	-	2.26 ng/mL	[S6]
Mab	icCLEIA	GTM	-	0.002 ng/mL	[S7]
CDs@SBA-15	Fluorescence detection	CTC	Turn off	113 nM	This work
MQDA–Eu^{3+}	Fluorescence detection	CTC	Turn off	0.93 μM	[S8]
N-CDs@MIPs	Fluorescence detection	CTC	Turn off	3.19 μM	[S9]
N-CDs	Fluorescence detection	CTC	Turn off	0.17 μM	[S10]
IO-QDs	Fluorescence detection	CTC	Turn off	120.23 nM	[S11]
JLUE–MOG–7	Fluorescence detection	CTC	Turn off	0.52 μM	[S12]
D-μSPE	HPLC-UV	CTC	-	7.0 μg/L	[S13]
-	UHPLC-MS/MS	CTC	-	11.3 μg kg^{-1}	[S14]

References

[S1] Zhou, Y.; Wang, J.; Zhao, Q.; Cai, H.; Zhang, H., Selective adsorption and removal of congo red based on ethylenediamine functionalized mesoporous silica. *ChemistrySelect* **2022**, *7*, e202203280.

[S2]Sajwan, R. K.; Solanki, P. R., A hybrid optical strategy based on graphene quantum dots and gold nanoparticles for selective determination of gentamicin in the milk and egg samples. *Food Chemistry* **2022**, *370*, 131312.

[S3] Sajwan, R. K.; Solanki, P. R., Gold@Carbon quantum dots nanocomposites based two-in-one sensor: a novel approach for sensitive detection of aminoglycosides antibiotics in food samples. *Food Chemistry* **2023**, *415*, 135590.

[S4] Long, X.; Liu, H.; Hu, J.; Wu, S., Green synthesis of N, S dual heteroatom-doped fluorescent carbon dots (N, S-CDs) and their applications in gentamicin sensing and dual-switch anti-counterfeiting encryption. *Dyes and Pigments* **2024**, *231*, 112413.

[S5] Dong, W.; Li, Z.; Wen, W.; Liu, B.; Wen, G., Novel CdS/MOF cathodic photoelectrochemical (PEC) platform for the detection of doxorubicin hydrochloride and gentamicin sulfate. *ACS Applied Materials & Interfaces* **2021**, *13*, 57497-57504.

[S6] Xia, Y.; Su, R.; Huang, R.; Ding, L.; Wang, L.; Qi, W.; He, Z., Design of elution strategy for simultaneous detection of chloramphenicol and gentamicin in complex samples using surface plasmon resonance. *Biosensors and Bioelectronics* **2017**, *92*, 266-272.

[S7] Dai, P.; Zhang, Y.; Hong, Y.; Xiong, J.; Du, H.; Duan, L.; Wang, D.; Wang, Y.; Deng, W.; Hammock, B. D.; Yang, W., Production of high affinity monoclonal antibody and development of indirect competitive chemiluminescence enzyme immunoassay for gentamicin residue in animal tissues. *Food Chemistry* **2023**, *400*, 134067.

[S8] Ran, J. M.; Yang, L.; Liu, C. T.; Liu, Q. H.; Liu, Y. L.; Li, S. J.; Fu, Y.; Ye, F., A novel fluorescence platform for specific detection of tetracycline antibiotics based on [MQDA-Eu^{3+}] system. *Science of The Total Environment* **2024**, *931*, 172866.

[S9] Ren, Y.; Fan, Z., Synthesis of molecularly imprinted polymers based on nitrogen-doped carbon dots for specific detection of chlortetracycline by reversed phase microemulsion method. *Talanta* **2023**, *265*, 124898.

[S10] Ma, L.; Liu, J.; Long, X.; Wu, S., Green synthesis of fluorescent carbon dots from waste chicken feathers for chlortetracycline sensing. *Journal of Molecular Structure* **2025**, *1319*, 139444.

[S11] Sudewi, S.; Zulfajri, M.; Dayalan, S.; Hsu, S. C. N.; Huang, G. G., Glutamic acid–capped iron oxide quantum dots as fluorescent nanoprobe for tetracycline in urine. *Microchimica Acta* **2023**, *190*, 226.

[S12] Liu, M.; Liu, Z.; Ma, T.; Liu, Z.; Li, Y.; Zou, D., Luminescent cellulose-based porous binary metal-organic gels in an adsorption bed for effective adsorption and sensitive detection of chlortetracycline hydrochloride. *Journal of Hazardous Materials* **2021**, *414*, 125473.

[S13] Nilnit, T.; Jeenno, J.; Supharoek, S. a.; Vichapong, J.; Siriangkhawut, W.; Ponhong, K., Synergy of iron-natural phenolic microparticles and hydrophobic ionic liquid for enrichment of tetracycline residues in honey prior to HPLC-UV detection. *Food Chemistry* **2024**, *437*, 137879.

[S14] Vergara Luis, I.; Báez Millán, J. C.; Baciero, I.; González Gaya, B.; Olivares, M.; Zuloaga, O.; Prieto, A., Comparison of conventional and dispersive solid phase extraction clean-up approaches for the simultaneous analysis of tetracyclines and sulfonamides in a variety of fresh vegetables. *Talanta* **2023**, *254*, 124192.

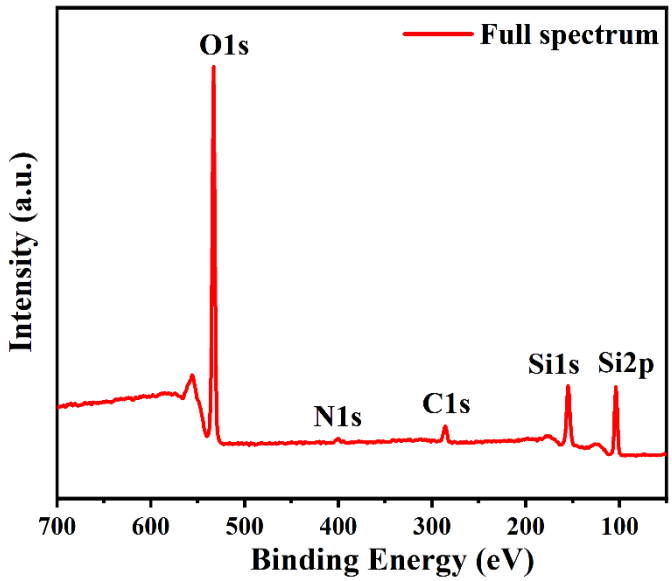

Fig. S1 XPS full spectrum.

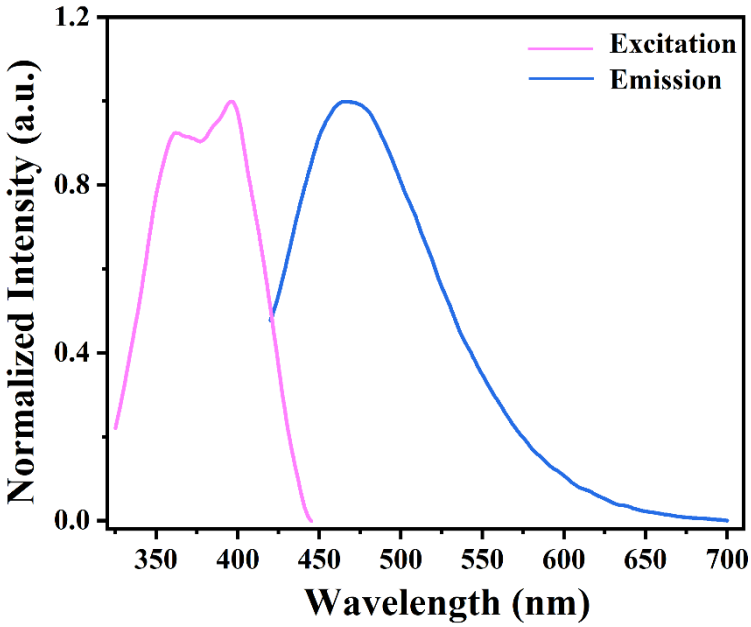

Fig. S2 Normalized fluorescence excitation and emission spectra of CDs@SBA-15.

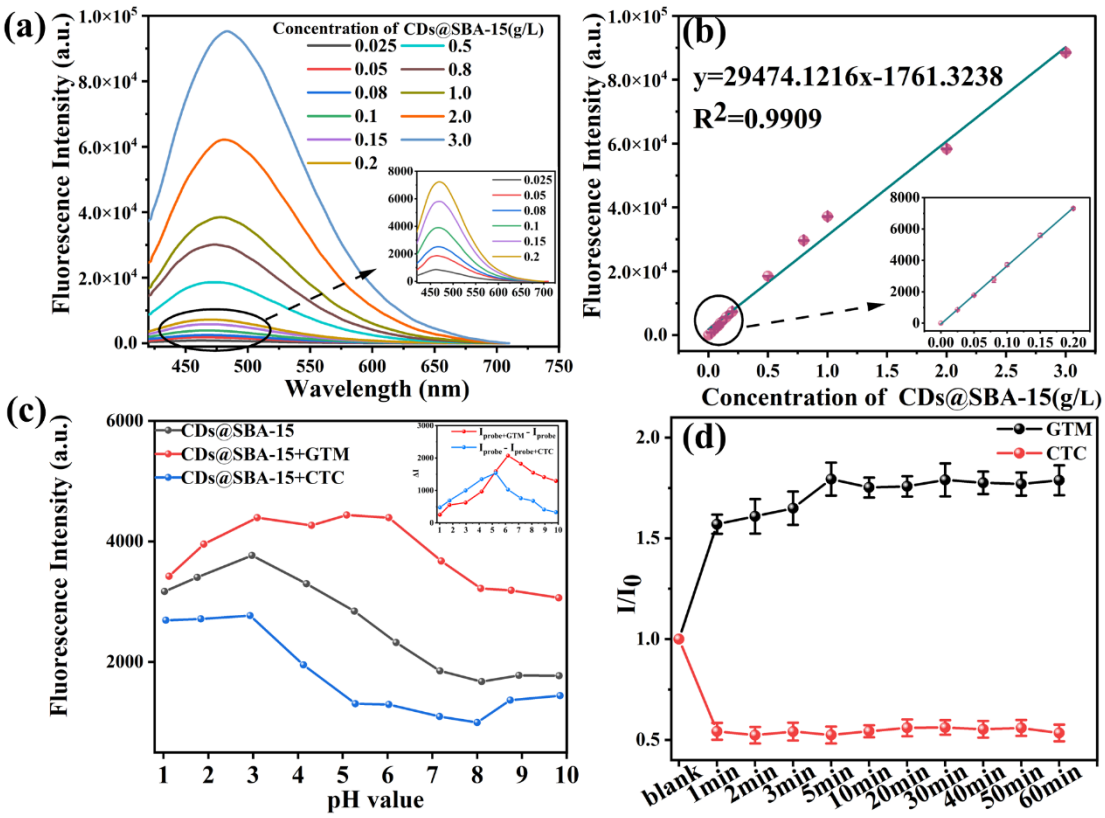

Fig. S3 Fluorescence spectra (a) and linear plots (b) of CDs@SBA-15 probe at different concentrations (0.025 g/L-3.0 g/L); effect of pH (c) (inset shows ΔI before and after the addition of GTM or CTC) and time (d) on the detection of GTM/CTC (100 μM)

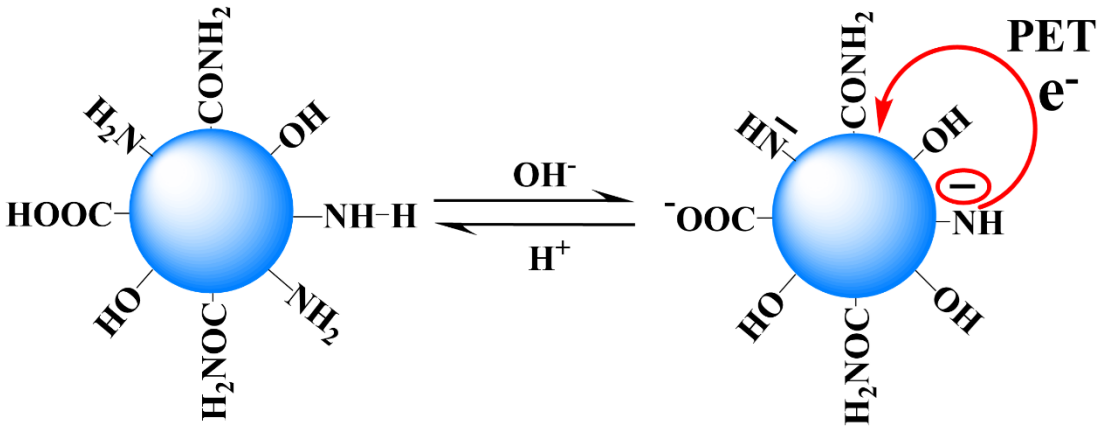

Fig. S4 PET behavior on CDs.

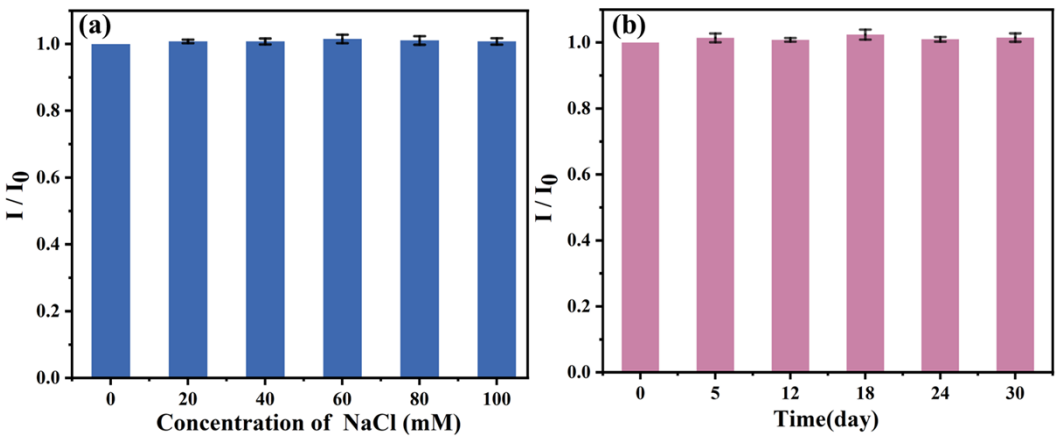

Fig. S5 Effect of ionic strength (a) and storage time (b) on CDs@SBA-15.

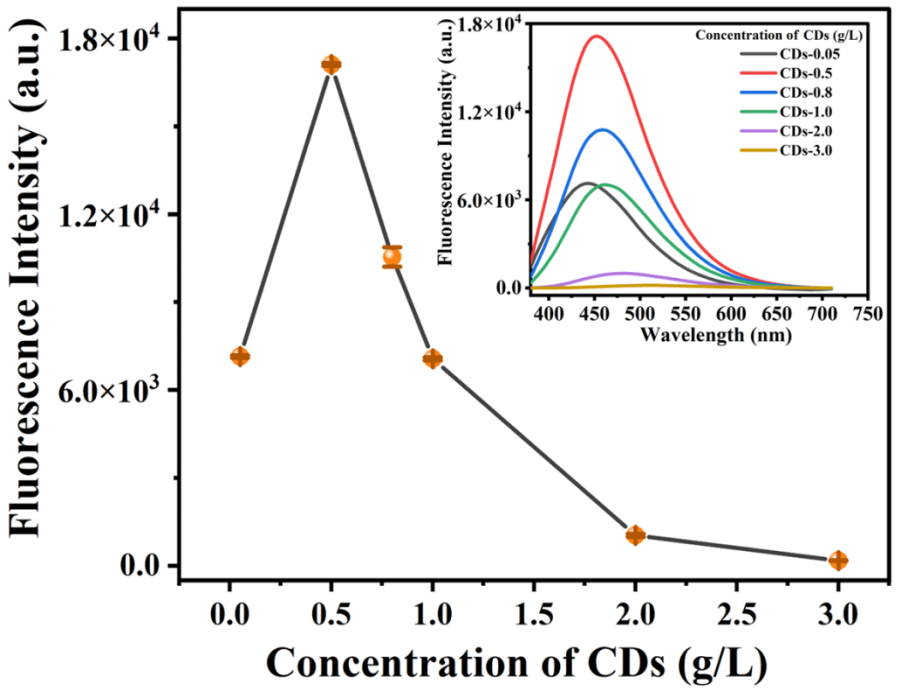

Fig. S6 Relationship between maximum emission peak and the concentrations of CDs (inset shows fluorescence spectra of CDs).

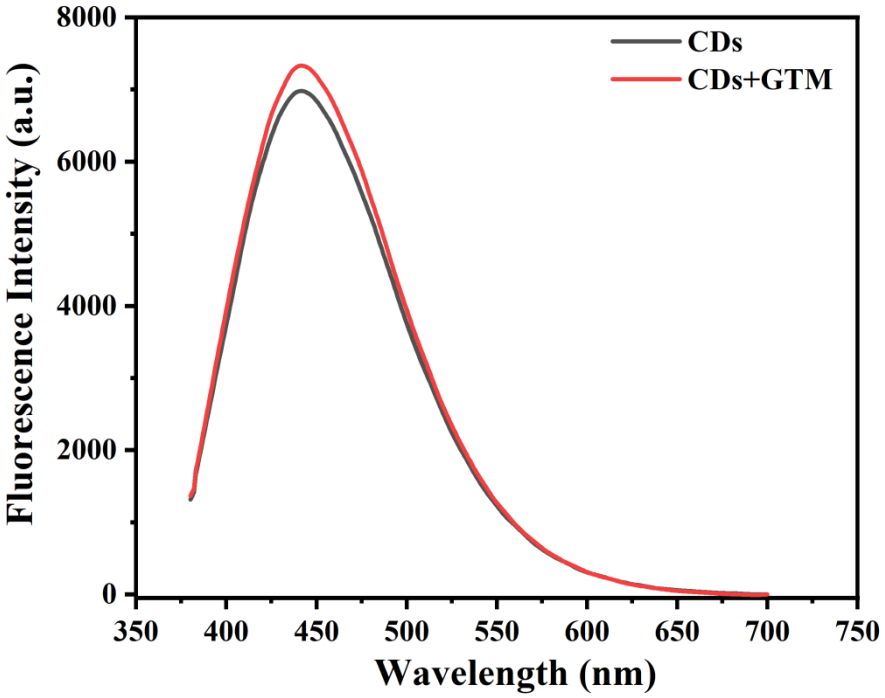

Fig. S7 Fluorescence spectra of CDs before and after the addition of GTM (100 μM).

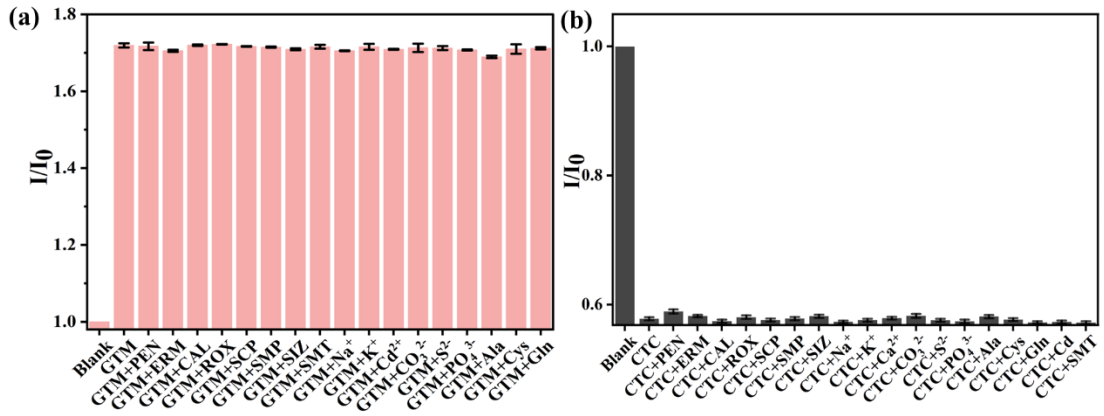

Fig. S8 Fluorescence intensity ratio (I/I_0) of CDs@SBA-15 in the presence of GTM (a) or CTC (b) and each of the interfering substances.

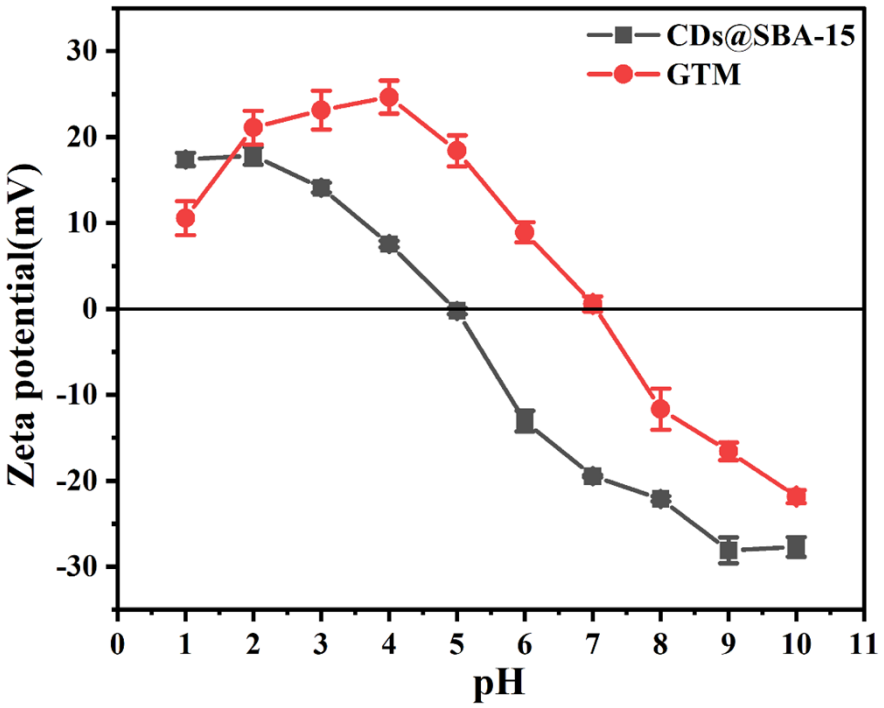

Fig. S9 The zeta potential of CDs@SBA-15 and GTM.

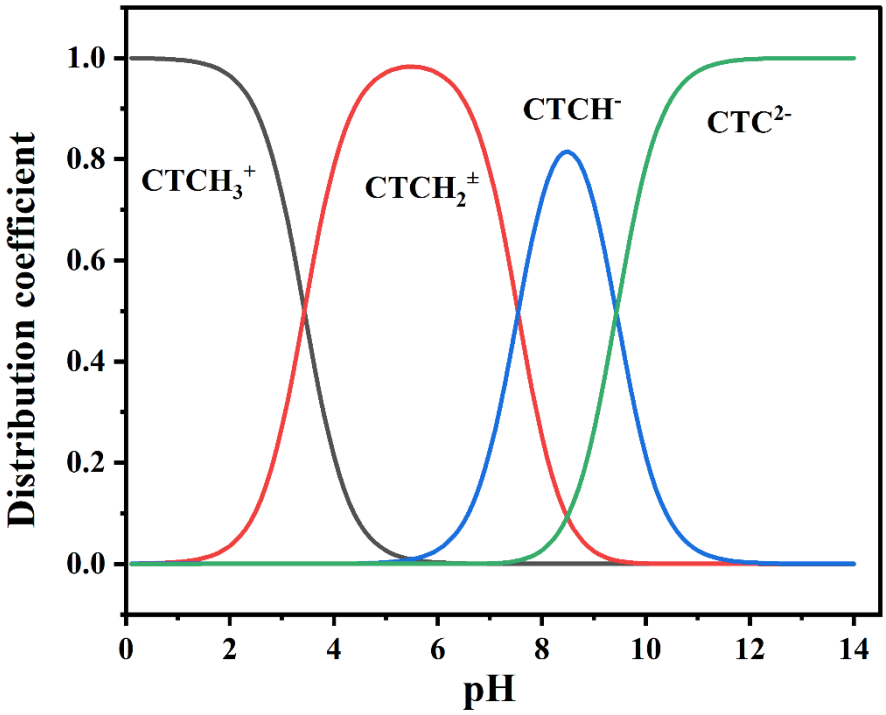

Fig. S10 Plot of CTC distribution coefficients.

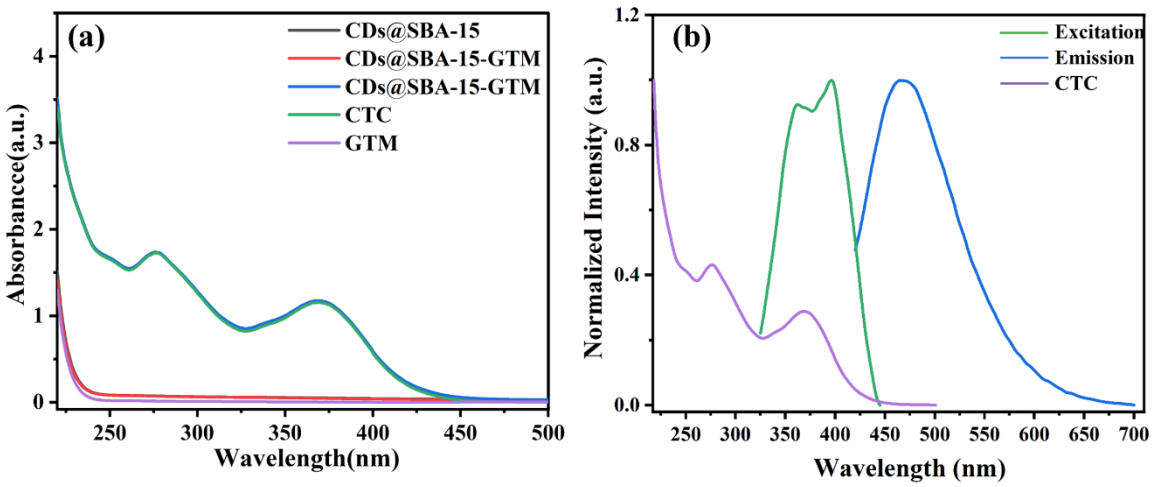

Fig. S11. (a) UV–vis absorption spectra of CTC, GTM and CDs@SBA-15 in the absence and presence GTM and CTC. (b) UV–Vis absorption spectra of CTC and the excitation and emission spectra of the nanoprobe.

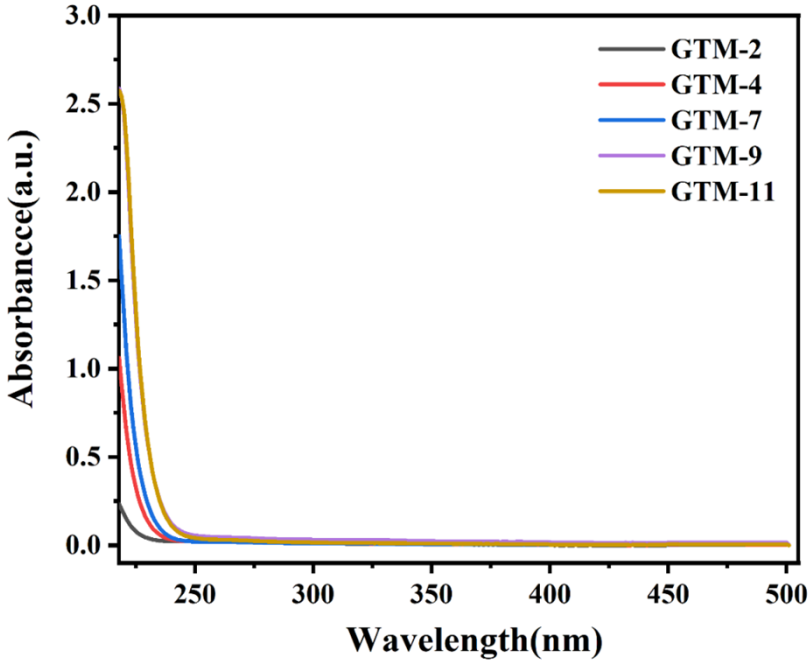

Fig. S12 UV absorption spectrum of GTM at pH = 2 – 11.

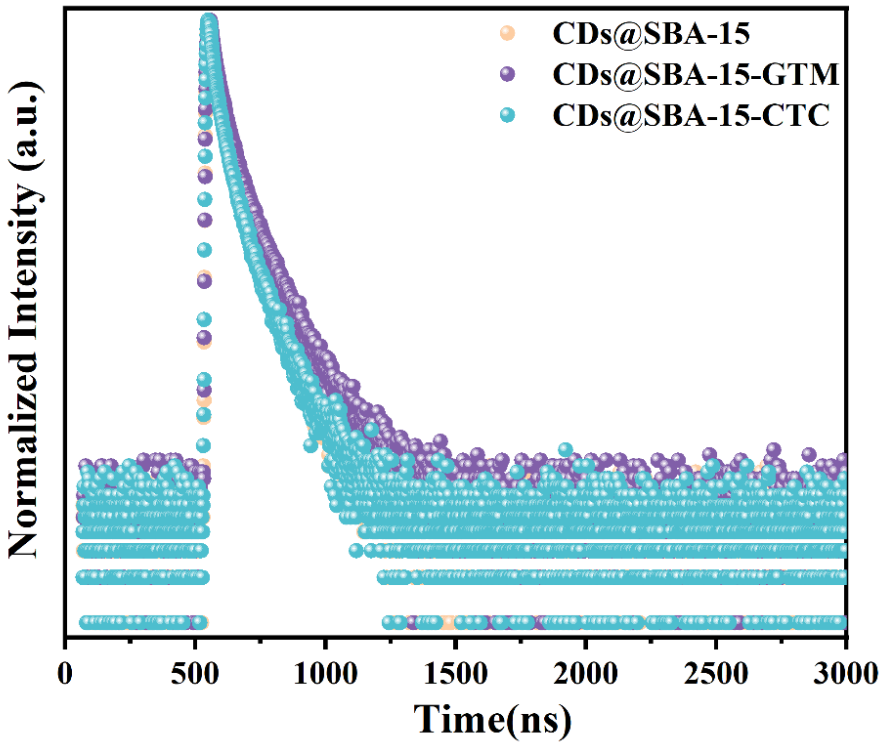

Fig. S13 fluorescence decay curve of CDs@SBA-15 in the absence and presence GTM and CTC.

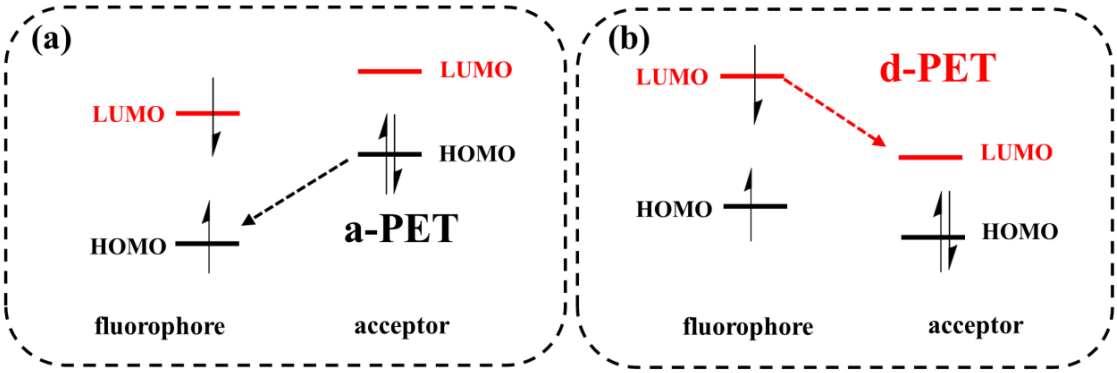

Fig. S14 PET mechanism: (a) a-PET and (b) d-PET processes.

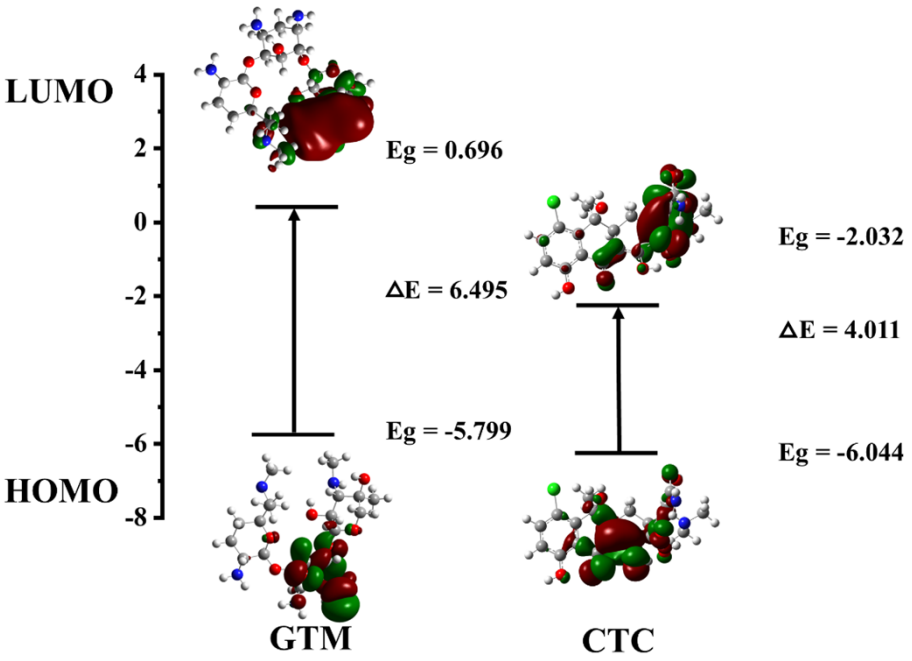

Fig. S15 LUMO-HOMO energy level diagrams for GTM and CTC.

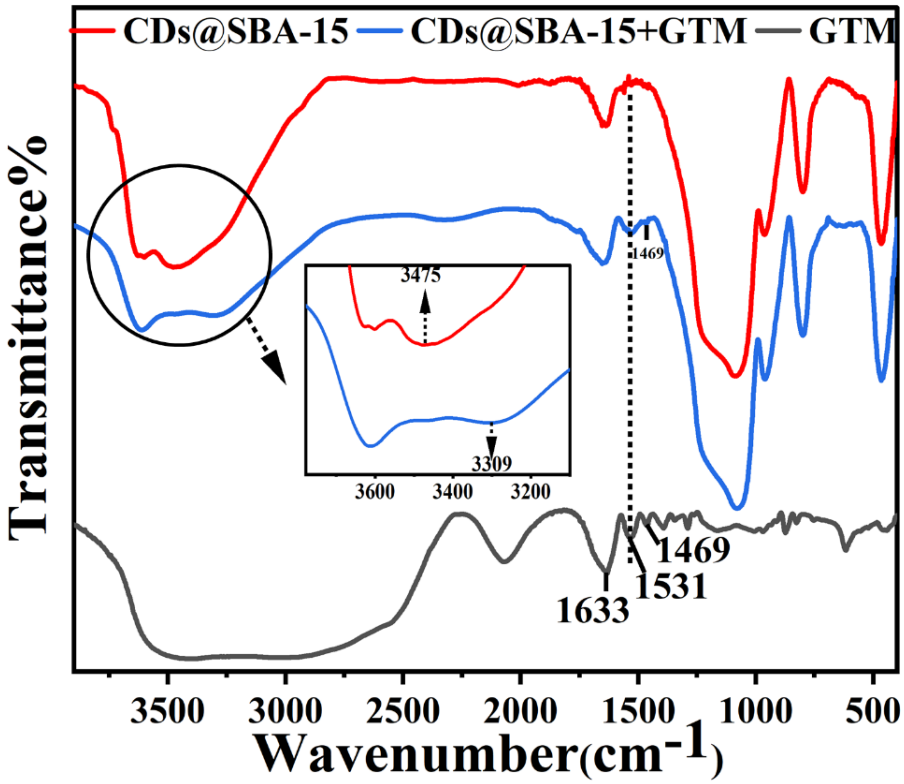

Fig. S16 FT-IR spectra of CDs@SBA-15, CDs@SBA-15+GTM and GTM.

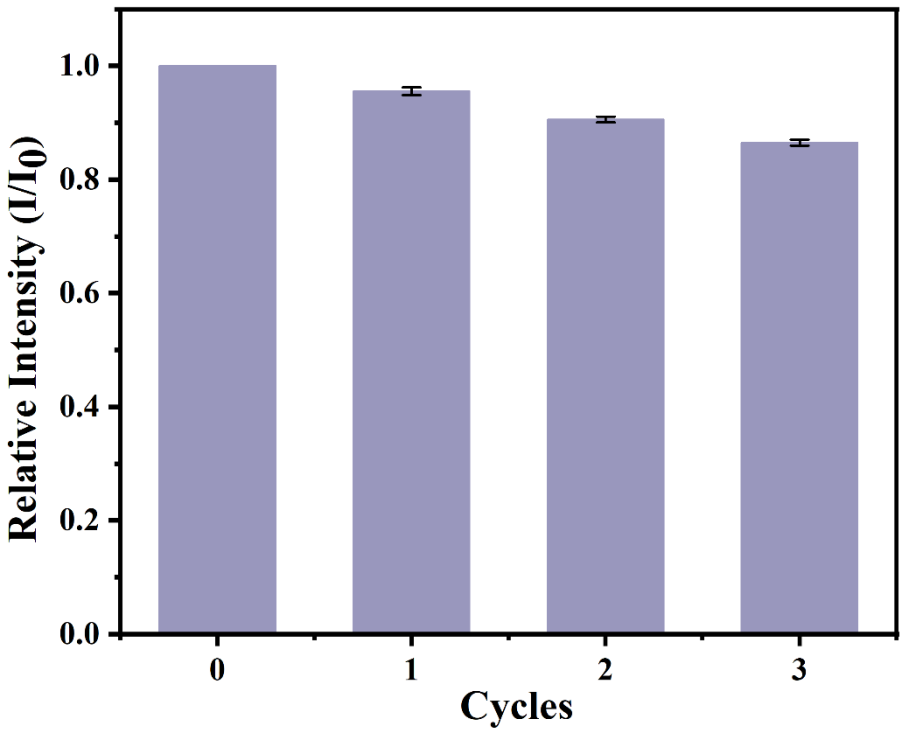

Fig. S17 Recovery performance of CDs@SBA-15 for GTM (100 μM) detection.